

ORIGINAL ARTICLE

ATF6 α promotes prostate cancer progression by enhancing PLA2G4A-mediated arachidonic acid metabolism and protecting tumor cells against ferroptosis

Ru Zhao MD¹  | Ye Lv MD² | Tingting Feng PhD¹ | Ruoja Zhang MD³ |
Luna Ge PhD^{3,4} | Jihong Pan PhD^{3,4} | Bo Han PhD¹  | Guanhua Song PhD⁵ |
Lin Wang PhD^{3,4}

¹Department of Pathology, Shandong University Medical School, Jinan, China

²Shandong Provincial Key Laboratory of Animal Resistance Biology, College of Life Sciences, Shandong Normal University, Jinan, China

³Key Lab for Biotech-Drugs of National Health Commission, Key Lab for Rare & Uncommon Diseases of Shandong Province, Biomedical Sciences College & Shandong Medicinal Biotechnology Centre, Shandong First Medical University & Shandong Academy of Medical Sciences, Jinan, China

⁴Department of Oncology, The First Affiliated Hospital of Shandong First Medical University, Jinan, China

⁵Institute of Basic Medicine, Shandong First Medical University & Shandong Academy of Medical Sciences, Jinan, China

Correspondence

Guanhua Song, PhD, Institute of Basic Medicine, Shandong First Medical University & Shandong Academy of Medical Sciences, #6699, Qingdao Rd, 250017 Jinan, China.
Email: yysghyy@163.com

Lin Wang, PhD, Key Lab for Biotech-Drugs of National Health Commission, Key Lab for Rare & Uncommon Diseases of Shandong Province, Biomedical Sciences College & Shandong Medicinal Biotechnology Centre, Shandong First Medical University & Shandong Academy of Medical Sciences, #6699, Qingdao Rd, 250017 Jinan, China.
Email: kecheng1216@163.com

Funding information

The Innovation Project of Shandong Academy of Medical Sciences, Grant/Award Number: 2022; The Youth Innovation Technology Plan of Shandong University, Grant/Award Number: 2019KJK003; The Natural Science Foundation of Shandong Province, Grant/Award Numbers: ZR2020YQ55, ZR2020QH327; Academic promotion program of Shandong First Medical University, Grant/Award Number: LJ001; Taishan Scholar Project of Shandong Province, Grant/Award Number: tsqn20161076;

Abstract

Background: Despite the clinical success of androgen receptor (AR)-targeted therapies, prostate cancer (PCa) inevitably progresses to castration-resistant prostate cancer (CRPC). Transcription factor 6 α (ATF6 α), an effector of the unfolded protein response (UPR) that modulates the cellular response to endoplasmic reticulum (ER) stress, has been linked to tumor development, metastasis, and relapse. However, the role of ATF6 α in CRPC remains unclear.

Methods: The effect of ATF6 α on the CRPC-like phenotype in PCa cells was evaluated by 3-(4,5-dimethylthiazol-2-yl)-5-(3-carb-Oxymethoxyphenyl)-2-(4-sulfophenyl)-2H-tetrazolium inner salt (MTS), 5-Bromo-2-deoxyUridine (BrdU) incorporation analysis, and cell death assay. Mechanistically, bioinformatic analysis was utilized to evaluate the potential of PLA2G4A as the target of ATF6 α . Moreover, Western blot analysis, real-time polymerase chain reaction, chromatin immunoprecipitation, arachidonic acid (AA), and prostaglandin E2 (PGE2) assays were performed to identify the regulatory effect of ATF6 α on PLA2G4A.

Results: In this study, we found that the increase of ATF6 α expression in response to androgen deprivation generates PCa cells with a CRPC-like phenotype. PCa cells with high levels of ATF6 α expression are resistant to ferroptosis, and genetic and pharmacological inhibition of ATF6 α could, therefore, promote the ferroptotic death of tumor cells and delay PCa progression. Molecular analyses linked ATF6 α regulation of

Ru Zhao and Ye Lv contributed equally to this study.

This is an open access article under the terms of the Creative Commons Attribution-NonCommercial-NoDerivs License, which permits use and distribution in any medium, provided the original work is properly cited, the use is non-commercial and no modifications or adaptations are made.

© 2022 The Authors. *The Prostate* published by Wiley Periodicals LLC

National Natural Science Foundation of China, Grant/Award Numbers: 81772760, 82072850

ferroptosis to the PLA2G4A-mediated release of AA and the resulting increase in PGE2 production, the latter of which acts as an antiapoptotic factor.

Conclusions: This study defines ATF6 α as a novel antiapoptotic regulator that exacerbates PCa progression. In addition, our data establish ATF6 α -PLA2G4A signaling as an important pathological pathway in PCa, and targeting this pathway may be a novel treatment strategy.

KEYWORDS

AA, ATF6 α , CRPC, ferroptosis, PGE2, PLA2G4A

1 | INTRODUCTION

Prostate cancer (PCa) development and progression are largely dictated by androgen receptor (AR) action; therefore, androgen deprivation therapy (ADT) has remained the frontline strategy for clinical management. However, all patients will ultimately relapse with incurable castration-resistant prostate cancer (CRPC).¹ Previous studies demonstrated that lipid metabolism was altered during the development of CRPC, and an increase in intratumoral essential polyunsaturated fatty acids (PUFAs) was observed.^{2,3} Furthermore, dysregulation of lipid homeostasis is a metabolic hallmark associated with PCa tumorigenesis and disease progression to CRPC in response to ADT.⁴ This rewiring of lipid metabolism offers new therapeutic opportunities and has led to the development of multiple inhibitors, which are promising for PCa treatment.

As an important cellular protective response to excess intracellular lipid peroxides, ferroptosis is a nonapoptotic form of regulated cell death that is characterized by enhanced peroxidation of phospholipids enriched with PUFAs and reactive oxygen species in an iron-dependent manner.^{5,6} At the molecular level, the antioxidant enzyme glutathione peroxidase 4 (GPX4) uses reduced glutathione to convert phospholipid hydroperoxides to lipid alcohols and consequently inhibits ferroptosis.^{7,8} Accumulating evidence indicates that ferroptosis is involved in tumorigenesis and progression and can act as a natural barrier to tumor progression. In cancer, ferroptosis inducers, such as erastin and RSL3, which inhibit GPX4 and cystine/glutamate transporters composed of SLC7A11 and SLC3A2, exhibit promising anticancer activity in multiple cancer types.^{9,10} Previous studies have shown that drug-resistant cancer cells are vulnerable to GPX4 inhibition and ferroptosis induction.^{11,12} Moreover, induction of ferroptosis enhances the therapeutic efficacy of cisplatin in cancer cells.^{13,14} In the context of PCa, tumor cells are vulnerable to ferroptosis induction, and treatment with the antiandrogen enzalutamide induces lipid peroxidation and leads to sensitivity to GPX4 inhibition and ferroptosis.^{4,15} Therefore, ferroptosis is closely related to PCa progression, and ferroptosis inducers may be even more potent in combination therapy settings.

In cancer, the accumulation of misfolded or unfolded proteins can disrupt the balance of endoplasmic reticulum (ER) homeostasis and induce ER stress. The unfolded protein response (UPR) could be subsequently activated to help cancer cells cope with ER stress. Thus, the ER stress response in this setting could be a cytoprotective response with an

important role in tumor growth, especially in tumors arising from active secretory cells.^{16,17} The UPR signaling pathway is mainly composed of inositol-requiring enzyme 1 (IRE1), activating transcription factor 6 (ATF6 α), and protein kinase RNA-like ER kinase (PERK). In particular, PCa cells may have developed ways to engage ER adaptive responses and hormonally regulate the UPR to support prostate tumorigenesis.¹⁸ Importantly, a previous study demonstrated that ferroptotic inducers could activate the ER stress-mediated PERK-eIF2 α -ATF4-CHOP cascade without inducing apoptosis.¹⁹ Therefore, elucidating the interconnection between ferroptosis and UPR may provide novel mechanistic insight into the pathological progression of PCa and an additional treatment strategy.

In this study, we found that PCa cells with ATF6 α overexpression demonstrated a CRPC-like phenotype. Critically, RNA sequencing (RNA-seq) and molecular analysis revealed that ATF6 α -PLA2G4A mediated regulation of arachidonic acid (AA) metabolism as an adaptive survival response against ferroptosis that may contribute to the emergence of CRPC. Furthermore, the ATF6 α inhibitor Ceapin-A7 may represent a new class of therapeutic agents for advanced PCa as a single agent and in combination with standard-of-care therapy for CRPC.

2 | MATERIALS AND METHODS

2.1 | Cell culture and reagents

The human prostate cancer cell lines LNCaP, C4-2B, VCaP, PC3 were purchased from the American Type Culture Collection and cultured following ATCC's instructions. The LNCaP-AI cells were established by culturing the LNCaP cells in media with 10% charcoal-stripped fetal bovine serum (CSS; Hyclone). Ceapin-7 and A-23187 was purchased from Sigma. All cells were maintained at 37°C in a humidified incubator with 5% CO₂. RSL3, ML210, ferrostatin-1, liproxstatin-1, zVAD-fmk, necrostatin-1, Erastin, PAF, and Enzalutamide were purchased from Selleck Chemicals.

2.2 | Generation of ATF6 α -/-PCa cells

The clustered regularly interspaced short palindrome repeats/CRISPR-associated protein 9 (CRISPR/Cas9) system (PSPCas9(BB)

-2A-Puro; PX459) was purchased from Addgene. LentiCRISPR v2-sg ATF6 α (GenePharma) was used to knockout ATF6 α . Knockout cells were generated according to a previous report.²⁰ After about 2 weeks' drug selection, puro-resistant clones were manually picked and transferred to a 96-well plate for further expansion. Correctly gene-targeted clones were identified by real-time polymerase chain reaction (qRT-PCR) and Western blot analysis.

2.3 | RNA isolation and qRT-PCR

Total RNA extraction and qRT-PCR were performed as previously described.²¹ The details of the primers of genes are listed in Table S1. GAPDH was used as internal loading controls. The relative expression quantity was calculated using the $2^{-\Delta\Delta C_t}$ method. Each sample was analyzed in triplicate.

2.4 | Western blot analysis

Western blot analysis was performed as previously described.²¹ Primary antibodies for ATF6 α (Abcam), β -actin (Abcam), GPX4 (Abcam), PLA2G4A (Santa Cruz Biotechnology), and secondary antibody (Abcam) were applied according to the manufacturer's instructions.

2.5 | Cell transfection

ATF6 α and PLA2G4A overexpression and empty control plasmids were purchased from Vigene. Human Lenti-ATF6 α -EGF and its control Lenti-EGFP were obtained from Genecopoeia. The siRNAs were designed and synthesized by RiboBio and was used at a concentration of 100 nM. To avoid off-target effects, cotransfection of two RNAs with better interference efficiency was performed. Nonspecific negative control siRNAs (NC) were used (sense strand: 5'-UUCUCCGAACGUGUCACG-3'; anti-sense strand: 5'-ACGUGACACG UUCGGAGAATT-3'). Cells were transfected with the oligonucleotide using Lipofectamine 2000 (Invitrogen LifeTechnologies) following the manufacturer's instructions and all experiments were performed 24–48 h after transfection. Cell viability was then analyzed by 3-(4,5-dimethylthiazol-2-yl)-5-(3-carb-Oxymethoxy phenyl)-2-(4-sulfophenyl)-2H-tetrazolium inner salt (MTS) (Promega) and quantification of cell death was confirmed by propidium iodide staining followed by fluorescence activated cell sorting analysis as previously described.²²

2.6 | Chromatin immunoprecipitation assay (ChIP)

The ChIP assay was performed using Magna ChIP™ Kit (MerckMillipore) following the manufacturer's protocol. ChIP assay was performed as previously described.²¹ Chromatin from cells was fixed and immunoprecipitated using 2 mg of anti-ATF6 α , anti-Histone H3 (trimethyl K27) (Abcam), anti-Histone H3 (acetyl K9) (Abcam), or

irrelevant antibody (anti-IgG, Santa Cruz Biotechnology). The purified and eluted DNA fragments were then quantified by qRT-PCR assays. The primers are listed in Table S1.

2.7 | Dual-luciferase assay

The cells transfected with indicated plasmid or siRNA were harvested and subjected to luciferase reporter assay using the dual-luciferase assay reporter system (Promega) according to the manufacturer's instructions as previously described.²³ In all cases, 40 ng/well of pHRL-TK reporter gene was cotransfected to normalize the data for the transfection efficiency. Data are expressed as the mean fold induction \pm s.e.m. relative to control levels from a minimum of three separate experiments.

2.8 | AA and prostaglandin E2 (PGE2) assay

Cells were cultured and stimulated as described above, and supernatants were collected at the indicated time points. AA and PGE2 concentrations in the supernatant were analyzed using a commercial kit (R&D Systems) respectively according to the manufacturer's instructions.

2.9 | Determination of the labile iron pool and lipid peroxidation

The total cellular lipid peroxidation was measured using a C11 BODIPY (581/591) probe (Cayman Chemical) and the total cellular labile iron pool was detected based on the calcein-acetoxymethyl ester (C-AM) method as previously described.²⁴

2.10 | Mouse tumor xenograft model

Male nude mice (6 weeks old) were purchased from Weitonglihua Biotechnology and stayed in a specific pathogen-free environment. Mice were randomly split into two groups ($n = 5$ /group) including control and stable ATF6 α overexpression (or knockdown) groups. 6×10^6 cells in 150 μ l PBS were mixed with matrigel (1:1) and injected subcutaneously into the mice. To evaluate the therapeutic effect of the ATF6 α inhibitor, cells were injected subcutaneously into the mice. They were randomized into four groups ($n = 5$ /group) and treated as follows: vehicle control, enzalutamide, Ceapin-7, Ceapin-7+ enzalutamide. Tumor volume was monitored every 7 days, and tumor volume was calculated as follows: Volume = length \times (width)² \times 1/2. The mice were euthanized 7 weeks after implantation, and then, tumors were harvested. All animal experimental protocol was approved by the Institutional Animal Care and Use Committee of Shandong First Medical University and Shandong Academy of Medical Sciences and all procedures were performed in compliance with the institutional guidelines.

2.11 | Microarray analysis

LNCaP-AI cells were transfected with ATF6 α siRNA or negative control siRNA for 48 h. Then, total RNA was extracted by the TRIzol method to construct a cDNA library for RNA transcriptome sequencing by LC-BIO Technologies Co., Ltd. The top genes regulated by ATF6 α included genes that were up- or downregulated by >2-fold upon ATF6 α knockdown, and these genes were identified by the R package edgeR (<https://bioconductor.org/packages/release/bioc/html/edgeR.html>). Gene Ontology (GO) enrichment analysis and Kyoto Encyclopaedia of Genes and Genomes (KEGG) pathway enrichment analysis were used to evaluate the distribution of biological activities and signaling pathways among the differentially expressed genes. Gene set enrichment analysis (GSEA) was performed according to the manufacturer's instructions (<http://software.broadinstitute.org/gsea/index.jsp>).

2.12 | Statistical analysis

All data are presented as the mean \pm standard deviation (SD). SPSS software (version 20.0) was used to perform statistical analysis. Gene expression correlations were performed by Pearson's correlation analysis. Data were analyzed with two-tailed Student's *t* test, Mann-Whitney *U* test, and χ^2 test. *p* values < 0.05 were considered to be statistically significant.

3 | RESULTS

3.1 | Overexpression of ATF6 α results in a CRPC-like phenotype

To evaluate the functional impact of ATF6 α in CRPC, we used an isogenic pair of cell lines, LNCaP (androgen-responsive) and LNCaP-AI (androgen-independent). LNCaP-AI cells displayed higher expression of ATF6 α at both mRNA and protein levels than the parental LNCaP cells (Figure 1A). As shown by MTS (Figure 1B) and 5-Bromo-2-deoxyUridine (BrdU) incorporation assays (Figure 1C), knockdown of ATF6 α in LNCaP-AI cells (Figure S1A) delayed cell viability and proliferation in charcoal-stripped serum (CSS) media compared with those of its control cells. Similar effects were also found when LNCaP-AI cells were treated with ATF6 α -specific inhibitor Ceapin-A7 (Figure 1D,E). The effects of ATF6 α inhibition on cell viability and proliferation were also duplicated in C4-2B cells under androgen deprivation conditions (Figure S1B–E).

In contrast, ectopic expression of ATF6 α (Figure S1F) promoted the growth of LNCaP cells under hormone-free conditions *in vitro* (Figure 1F). To further explore these findings, we developed an *in vivo* xenograft mouse model using LNCaP with ATF6 α overexpression or not (Figure 1G). Importantly, LNCaP-ATF6 α -derived tumors grew more rapidly than the controls under castration conditions (118 ± 33.5 mm³/week vs. 30 ± 8 mm³/week) (Figure 1H), which was also confirmed by the weight (Figure 1I) of isolated tumors. In

contrast, shATF6 α in LNCaP-AI and C4-2B cells (Figure 1L,O) suppressed tumor growth under castration conditions (38 ± 15.2 mm³/week vs. 95 ± 12.8 mm³/week, 20 ± 4.5 mm³/week vs. 55 ± 11 mm³/week) (Figure 1J,K,M,N).

To further elucidate the critical effect of AR signaling on the function of ATF6 α , we demonstrated that the increase in viability of LNCaP cells caused by ATF6 α overexpression could not be blocked after siAR (Figure S2A) and enzalutamide (Enz) treatment (Figure S2B) without androgen. Thus, AR signaling was not required for ATF6 α to promote CRPC progression. Importantly, ATF6 α did not disturb AR responsiveness to diverse ligands, such as Enz and DHT (Figure S2C), indicating a potential role in treatment resistance during PCa progression.

3.2 | Integrative genomics analyses reveal the potential activity of ATF6 α in PCa

To illustrate the mechanism by which ATF6 α promotes PCa progression, we conducted comprehensive transcriptome analyses of LNCaP-AI cells with or without ATF6 α knockdown (Figure S2D). KEGG pathway analysis revealed that most genes were enriched in the AA metabolic pathway (Figure 2A). Further, GSEA demonstrated that the AA metabolic target gene set was enriched for upregulation in the NC (negative control) group (Figure 2B,C). We also validated the RNA-seq data by individual qRT-PCR analysis of AA metabolism-related genes in which their expression was inhibited upon ATF6 α knockdown (Figure 2D).

3.3 | ATF6 α induces ferroptotic resistance in PCa cells

A previous study demonstrated that the release of AA, caused by the hydrolysis of membrane phospholipids, could increase the production of PGE₂, which was shown to prevent hemin-induced ferroptosis.²⁵ As the transcriptome analyses showed that ATF6 α was closely related to AA metabolism, we then analyzed the effect of ATF6 α on ferroptosis in PCa cells. The CRPC-like PCa cell line LNCaP-AI was more resistant to ferroptosis, as determined by analyzing cell viability upon treatment with RSL3, a GPX4 inhibitor (Figure 3A), than the androgen-sensitive PCa cell line LNCaP. Similar results were also observed when PCa cells were treated with another GPX4 inhibitor, ML210 (Figure 3B). Importantly, ferrostatin-1 and liproxstatin-1, two ferroptosis inhibitors, almost completely reversed the RSL3- or ML210-induced cell death. Furthermore, the specificity of RSL3-induced ferroptotic death was confirmed by negative responses to inhibitors of alternative death programs, the pan caspase inhibitor zVAD-fmk or the RIPK1 inhibitor necrostatin-1 (Figure 3C,D). Thus, CRPC-like PCa cells are more resistant to the induction of ferroptotic death.

Importantly, ATF6 α -deficient LNCaP-AI and C4-2B cells also displayed elevated levels of the lipid-detoxifying enzyme GPX4 (Figure 3E). Therefore, we treated ATF6 α -deficient LNCaP-AI and C4-2B cells or their parental controls with RSL3 to induce ferroptosis.

The ATF6 α -deficient PCa cells displayed increased sensitivity to GPX4 inhibition (Figure 3F). Cotreatment with either Trolox or liprostatin, two inhibitors of ferroptosis, rescued the decrease of proliferation in ATF6 α -deficient cells under RSL3 treatment (Figure 3F). We also measured the levels of labile iron pool and lipid peroxides in PCa cells with ATF6 α knocking down or overexpressing.

As expected, increased lipid peroxides and labile iron pool caused by ferroptotic inducers became more obvious when ATF6 α was knocked down simultaneously (Figure S3A,C), but could be attenuated by overexpressing ATF6 α (Figure S3B,D). Moreover, inhibition of ATF6 α by its catalytic inhibitor Ceapin-A7 sensitized these cells to ferroptosis induced by ML210 (Figure S3E).

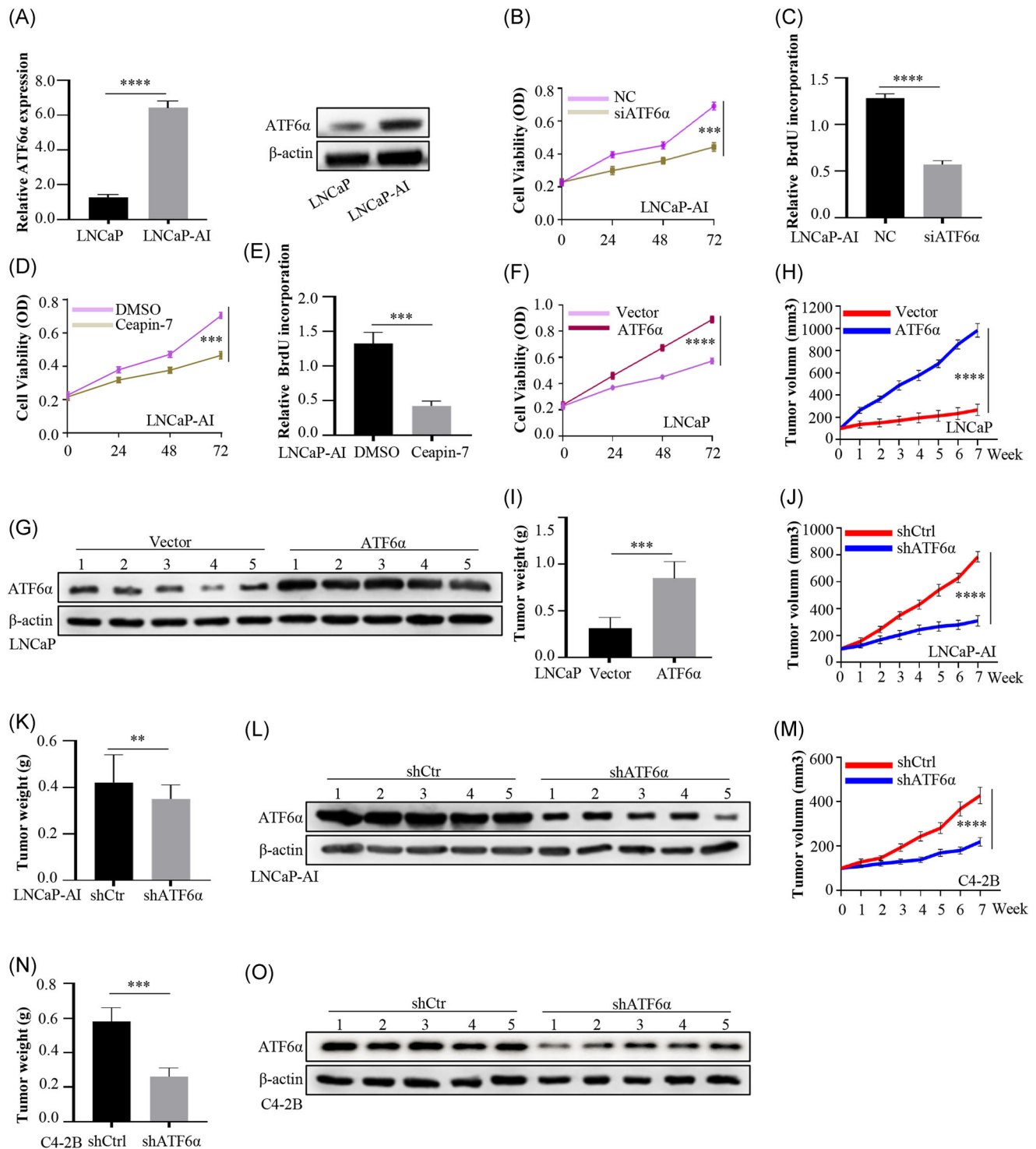


FIGURE 1 (See caption on next page)

Next, we asked whether the ectopic expression of ATF6 α in LNCaP and VCaP cells could diminish erastin-induced ferroptosis. As shown in Figure S3F, overexpression of ATF6 α abolished the erastin-induced growth inhibition in LNCaP and VCaP cells. A similar effect was also observed in ATF6 α -overexpressing LNCaP and VCaP cells upon the induction of ferroptosis by erastin (Figure S3G). These data imply that ATF6 α overexpression contributes to ferroptosis resistance in PCa cells.

Finally, we asked whether androgen deprivation affected ferroptosis. We found that ferroptotic death was further enhanced by androgen deprivation (Figure S4A) or enzalutamide (Figure S4B) treatment. However, this increase could be attenuated by overexpressing ATF6 α (Figure S4C). A similar tendency was also observed by characterizing GPX4 expression under the above experimental conditions (Figure S4D). Therefore, ATF6 α is closely related to ferroptosis in PCa.

3.4 | PLA2G4A as a target of ATF6 α -mediated transcriptional activation

Interestingly, the top-ranked gene among the ATF6 α knockdown-repressed genes is PLA2G4A, an enzymatic member of the cytosolic phospholipase A2 group IV family, which catalyzes the hydrolysis of membrane phospholipids to release AA and subsequently metabolize it into eicosanoids.²⁶ To verify that PLA2G4A is regulated by ATF6 α , we performed ATF6 α knockdown in multiple PC cell lines. qRT-PCR analysis using gene-specific primers showed that PLA2G4A expression was downregulated upon ATF6 α depletion in LNCaP-AI and C4-2B cells (Figures 4A and S4E). Consistent with this decrease in its mRNA levels, PLA2G4A protein expression was also strongly decreased, as demonstrated by Western blot analysis of LNCaP-AI and C4-2B cells (Figure 4B). Moreover, reintroduction of ectopic ATF6 α to these cells partially dampened the induction of PLA2G4A (Figure 4A,B), confirming the specificity of this regulation. Overall, our results indicate that ATF6 α is a transcriptional activator and suggest PLA2G4A as a definite target. Indeed, the direct regulation of PLA2G4A expression by ATF6 α was strengthened in

patients. PLA2G4A expression positively correlated with ATF6 α transcript levels in patient specimens (using data set GSE35988; Figure 4C).

We next investigated whether PLA2G4A is also a direct target of ATF6 α -mediated transcriptional activation. Analysis of ATF6 α ChIP-qPCR performed in LNCaP-AI cells identified strong ATF6 α binding at an enhancer approximately 1.2 kb upstream of the PLA2G4A gene promoter (Figure 4D). Furthermore, ATF6 α binding at this enhancer was decreased by 67% upon ATF6 α knockdown, supporting an authentic ATF6 α binding event. Similarly, ATF6 α occupied the same site in C4-2B cells (Figure 4D). In addition, ChIP-qPCR showed significantly enriched occupancy by active H3K9ac and the inactive histone mark H3K27me3 at the PLA2G4A promoter following ATF6 α knockdown, which was concordant with the decreased transcription of PLA2G4A (Figure S5A).

To further validate these observations, we carried out ATF6 α ChIP-qPCR analysis. Our data demonstrated that the PLA2G4A promoter showed a relatively weaker but still highly significant ATF6 α enrichment. Specifically, the presence of ATF6 α on the PLA2G4A promoter increased when ferroptosis was induced by erastin (Figure 4E) and RSL3 (Figure 4F) but decreased when erastin- and RSL3-induced ferroptosis was rescued by Trolox or liproxstatin. In addition, this change was accompanied by an obvious decrease in H3K9ac modifications and a concomitant increase in H3K27me3 levels (Figure S5B,C), suggesting that the loss of ATF6 α led to more condensed chromatin in the PLA2G4A gene locus and thereby blunted its transcription in PCa cells. Thus, our results indicate that ATF6 α is recruited to specific target loci in ferroptotic PCa cells, where it activates a transcriptional program that inhibits ferroptosis.

3.5 | ATF6 α activates PLA2G4A-mediated AA metabolism to maintain ferroptotic resistance in PCa cells

To analyze the role of ATF6 α in PLA2G4A-dependent AA release from cells, we inhibited ATF6 α in LNCaP-AI by treatment with siRNA (Figure S5D) or Ceapin-A7. The release of AA and

FIGURE 1 Effects of ATF6 α on PCa progression. (A) The expression levels of ATF6 α in LNCaP and LNCaP-AI cells were detected by qRT-PCR and Western blots. (B,C) Following the knockdown of ATF6 α in LNCaP-AI cells, cell viability was detected by MTS (B) and BrdU incorporation analysis (C). (D,E) After exposure to Ceapin-A7 (25 nM), the viability of LNCaP-AI cells was detected by MTS (D) and BrdU incorporation analysis (E). (F) Cell viability was evaluated by MTS assay after overexpressing ATF6 α in LNCaP cells under androgen-deprived conditions. (G–I) Nude mice were injected subcutaneously with either LNCaP-Vec Ctrl or LNCaP-ATF6 α cells and castrated once the tumors reached approximately 350 mm³. The protein levels of ATF6 α in tumor tissues formed by LNCaP-ATF6 α cells or its control in xenografts were measured by Western blot analysis (G). Tumor volumes formed by LNCaP-ATF6 α or its control in castrated mice were measured at the indicated weeks (H). The tumors were weighed at the seventh week (I). $n = 5$ in each group. (J–O) LNCaP-AI-shATF6 α (J–L) or C4-2B-shATF6 α cells (M–O) and their parental controls were injected into nude mice, which were castrated once the tumors reached approximately 300 mm³. The tumor volumes (J,M) and weight (K,N) were monitored at the indicated timepoint. $n = 5$ in each group. The protein levels of ATF6 α in tumor tissues formed by LNCaP-AI (L) and C4-2B (O) were measured by Western blot analysis. ATF6 α , activating transcription factor 6 α ; BrdU, 5-Bromo-2-deoxyUridine; MTS, 3-(4,5-dimethylthiazol-2-yl)-5-(3-carb-Oxymethoxyphenyl)-2-(4-sulfophenyl)-2H-tetrazolium inner salt; PCa, prostate cancer; qRT-PCR, quantitative real-time polymerase chain reaction. ** $p < 0.01$, *** $p < 0.001$, **** $p < 0.0001$, determined by two-tailed Student's *t* test [Color figure can be viewed at wileyonlinelibrary.com]

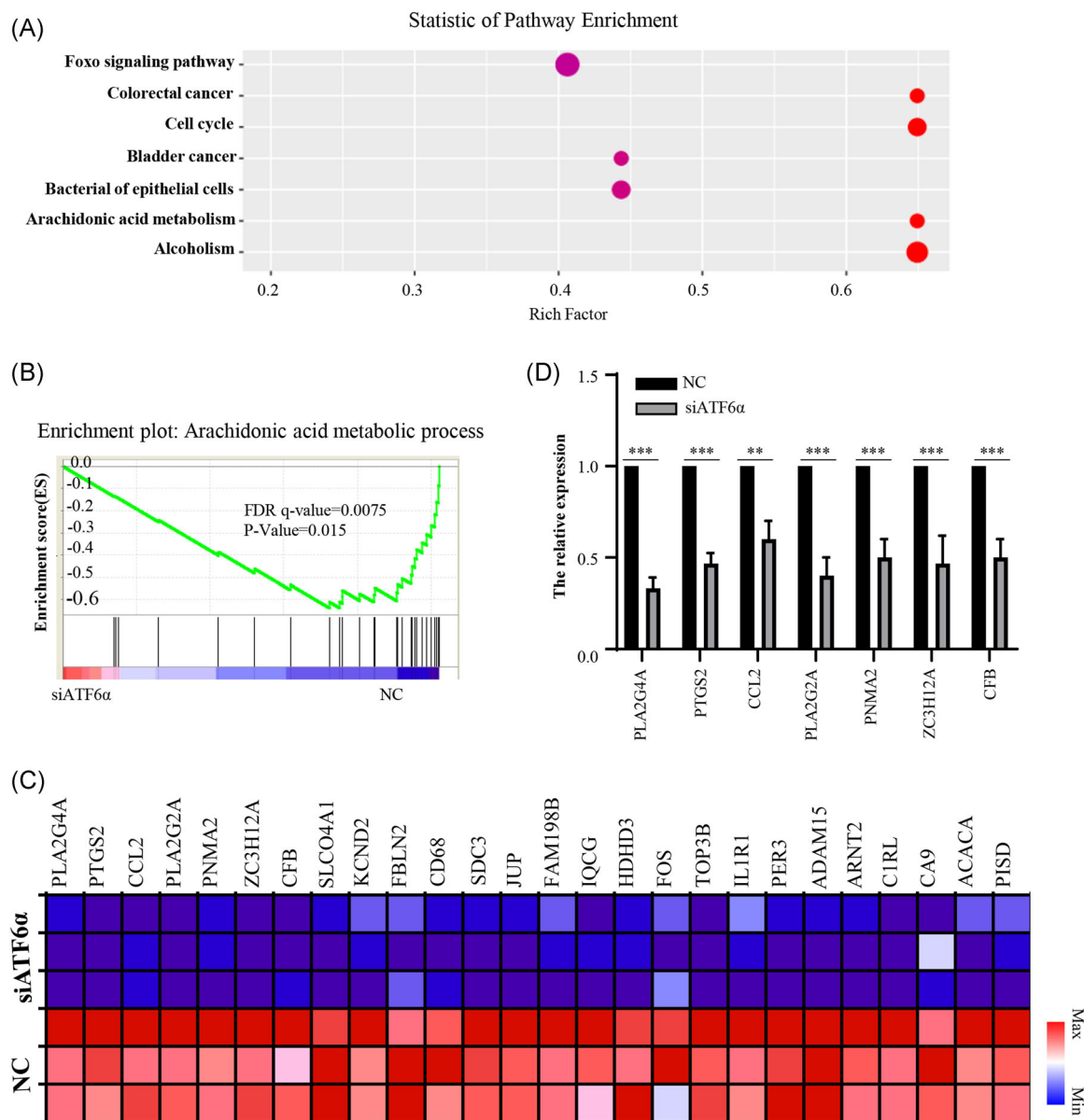


FIGURE 2 Prediction of ATF6α's potential activity in PCa using RNA sequencing. (A) ATF6α-related pathways were analyzed by KEGG analysis. (B) GSEA identified a significant association between ATF6α and the arachidonic acid metabolic pathway. (C) Heatmap of significant arachidonic acid metabolism-related genes in LNaP-AI cells with ATF6α knockdown compared with their parental controls. (D) The mRNA levels of the indicated genes were validated by qRT-PCR assays. ATF6α, activating transcription factor 6 α; GSEA, Gene set enrichment analysis; KEGG, Kyoto Encyclopaedia of Genes and Genomes; PCa, prostate cancer; qRT-PCR, quantitative real-time polymerase chain reaction. ** $p < 0.01$, *** $p < 0.001$, determined by two-tailed Student's t test [Color figure can be viewed at wileyonlinelibrary.com]

the resulting PGE₂ induced by 1 M A-23187 or 100 nM PAF was decreased in the siATF6α-transfected (Figure 5A,B) or Ceapin-A7-treated (Figure S6A,B) PCa cells. However, the reduced release of AA from the ATF6α-deficient PCa cells was rescued by overexpression of PLA2G4A.

PLA2G4A has primarily calcium-dependent phospholipase and lysophospholipase activities, with a major role in membrane lipid remodeling and biosynthesis of lipid mediators of the inflammatory response. As a key isoform of the group IV

phospholipase A₂ (PLA₂) family, this molecule can catalyze the release of AA for prostaglandin synthesis by cyclooxygenase 1 (PTGS1) and cyclooxygenase 2 (PTGS2). Importantly, PGE₂ could synergize with NAC to prevent hemin-induced ferroptosis.²⁶ Then, we asked whether PLA2G4A knockdown increases the sensitivity of PCa cells to proferroptotic challenge. The cell death triggered by RSL3 (Figure 5C) showed that PCa cells with PLA2G4A knockdown were more sensitive than their parental cells. To clarify the functional importance of the ATF6α/PLA2G4A axis,

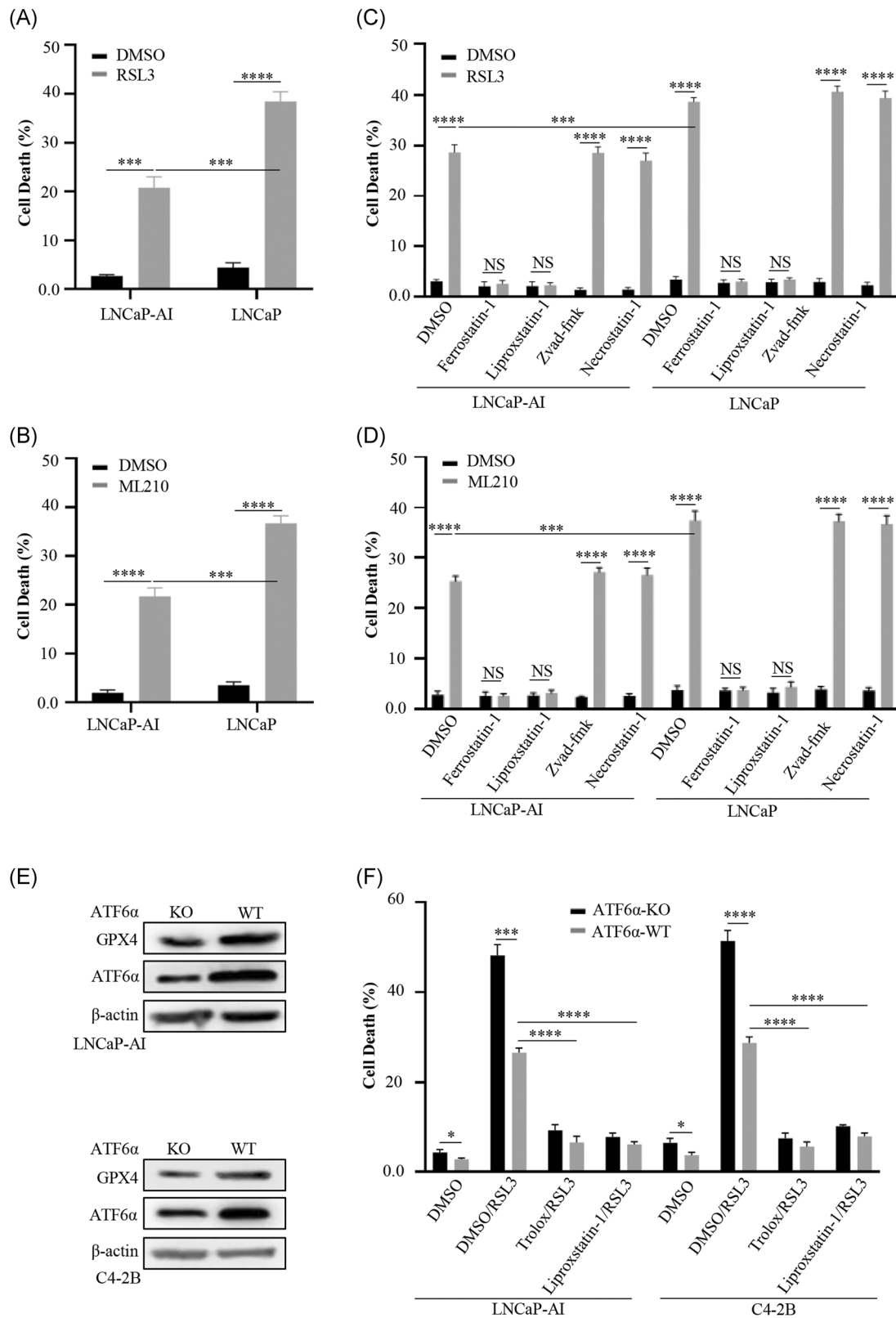


FIGURE 3 Effects of ATF6 α on ferroptosis in PCa. (A,B) Cell death was measured in LNCaP and LNCaP-AI cells after treatment with RSL3 (2 μ M, A) or ML210 (2 μ M, B) for 16 h. (C,D) With the induction of ferroptosis by RSL3 (C) or ML210 (D), cell death was measured in LNCaP and LNCaP-AI cells after treatment with ferrostatin-1 (10 μ M), liproxstatin-1 (1 μ M), zVAD-fmk (20 μ M), or necrostatin-1 (50 μ M). (E) Western blot analysis was performed to detect GPX4 and ATF6 α protein levels in LNCaP-AI and C4-2B cells with or without ATF6 α deficiency. (F) Cell death was measured in PCa cells with or without ATF6 α deficiency as indicated. ATF6 α , activating transcription factor 6 α ; PCa, prostate cancer. * p < 0.05, *** p < 0.001, **** p < 0.0001, determined by two-tailed Student's t test

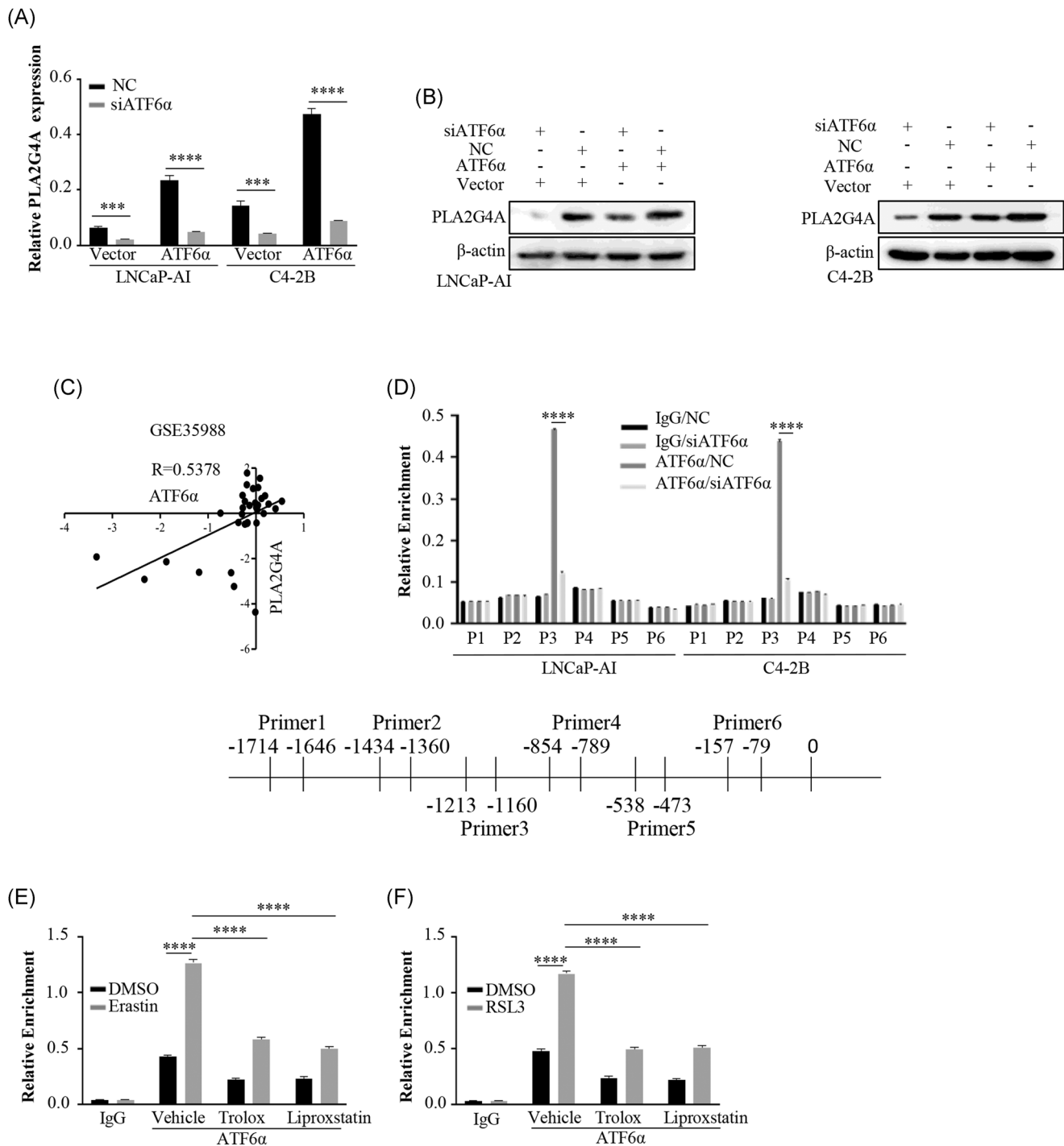


FIGURE 4 Effects of ATF6 α on PLA2G4A expression. (A,B) qRT-PCR (A) and Western blot analysis (B) were performed to detect the expression of PLA2G4A in PCa cells with ATF6 α overexpression or knockdown. (C) Correlation of ATF6 α and PLA2G4A expression in human PCa samples in a publicly accessible prostate cancer data set. (D) ATF6 α occupancy in the promoter of the PLA2G4A gene was detected by ChIP-PCR in LNCaP-AI and C4-2B cells. (E,F) LNCaP cells were pretreated with erastin (5 μ M, E) or RSL3 (2 μ M, F) and then treated with Trolox (100 μ M) or liproxstatin (1 μ M). ChIP-qPCR was performed to detect the presence of ATF6 α in the PLA2G4A gene. ATF6 α , activating transcription factor 6 α ; ChIP, Chromatin immunoprecipitation assay; PCa, prostate cancer; qRT-PCR, quantitative real-time polymerase chain reaction. *** p < 0.001, **** p < 0.0001, determined by two-tailed Student's t test

we depleted PLA2G4A expression in ATF6 α -overexpressing cells and found that PLA2G4A depletion diminished ferroptotic resistance in these cells to an extent similar to that of the control cells (Figure 5D).

Collectively, our results highlight that the ATF6 α /PLA2G4A cascade represents an important signaling pathway in PCa cells to strongly induce ferroptotic resistance and thereby promote PCa malignancy.

3.6 | Enzalutamide and Ceapin-A7 show synergistic effects in inhibiting PCa progression

A previous study demonstrated that inhibition of AR signaling by enzalutamide could induce lipid peroxidation and consequent ferroptosis. Ferroptosis inducers are a novel therapeutic approach for advanced PCa. Furthermore, PLA2G4A is required to sustain the activation of AR signaling in PCa. In the present study, we showed that the ATF6 α -PLA2G4A axis is closely related to ferroptosis in PCa. Thus, it may be beneficial to use ATF6 α inhibitors in conjunction with AR antagonists in CRPC.

To test this hypothesis, we treated CRPC-like PCa cells with enzalutamide, Ceapin-A7, or their combination. Cell growth assay revealed that Ceapin-A7 suppressed LNCaP-AI and C4-2B cell growth,

as expected, and strong synergistic effects of enzalutamide and Ceapin-A7 in the suppression of LNCaP-AI and C4-2B cell growth were found (Figure 6A). Importantly, we observed synergy between Ceapin-A7 and enzalutamide in inducing LNCaP-AI and C4-2B cell ferroptosis (Figure 6B). As we demonstrated synergistic effects of enzalutamide and Ceapin-A7 in suppressing PCa cell growth in vitro, we next investigated whether simultaneous treatment with Ceapin-A7 would sensitize CRPC tumors to enzalutamide in animal models. As expected, Ceapin-A7 in combination with Ceapin-A7 resulted in substantial tumor growth inhibition (Figure 6C,D).

In summary, these data demonstrated that inhibition of ATF6 α signaling using Ceapin-A7 enhanced the efficacy of enzalutamide in suppressing CRPC xenograft tumor growth.

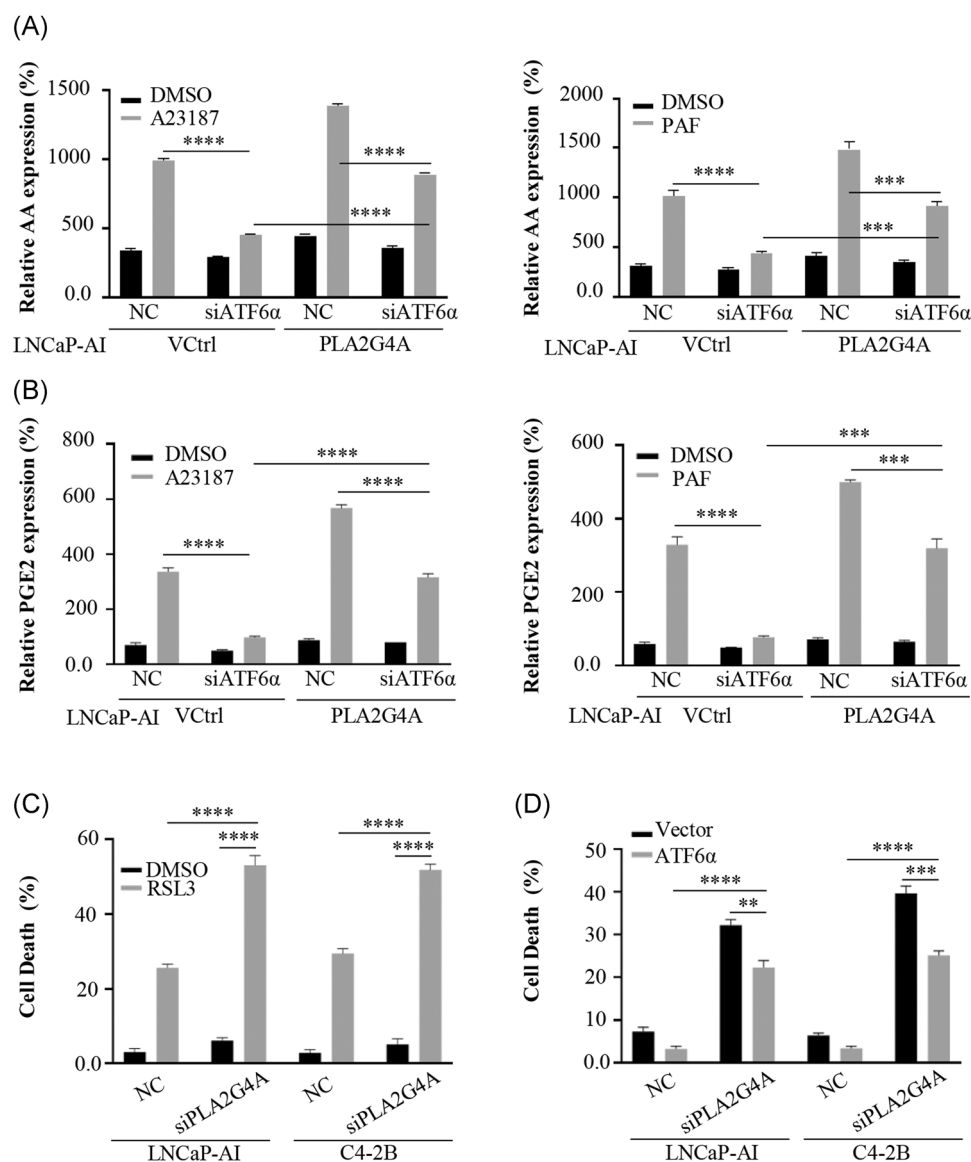


FIGURE 5 Effects of ATF6 α on the AA metabolic pathway. (A,B) The production of AA (A) and PGE2 (B) was measured in LNCaP-AI cells with or without ATF6 α knockdown and PLA2G4A overexpression. (C,D) With RSL3 (2 μ M) or ATF6 α overexpression, cell death was measured in LNCaP-AI cells with or without PLA2G4A knockdown. AA, arachidonic acid; ATF6 α , activating transcription factor 6 α ; PGE2, prostaglandin E2. ** p < 0.01, *** p < 0.001, **** p < 0.0001, determined by two-tailed Student's t test

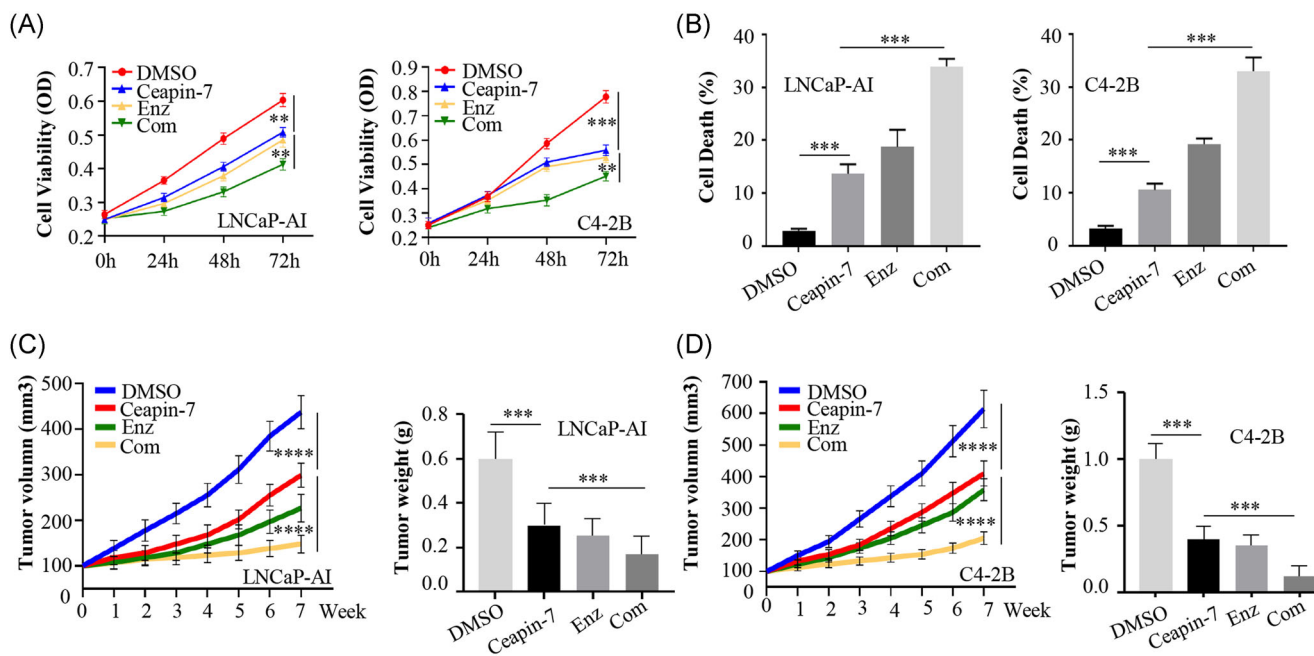


FIGURE 6 Effects of inhibiting both ATF6 α and AR signaling on PCa cells. (A,B) Cell viability and cell death of LNCaP-AI and C4-2B cells were detected by MTS and PI staining after treatment with Enz (1 μ M), Ceapin-A7 (25 nM) or in combination. (C,D) Tumor volume was measured in castrated nude mice after the indicated treatment. AR, androgen receptor; ATF6 α , activating transcription factor 6 α ; MTS, 3-(4,5-dimethylthiazol-2-yl)-5-(3-carb-Oxymethoxyphenyl)-2-(4-sulfophenyl)-2H-tetrazolium inner salt; PCa, prostate cancer; PI, propidium iodide. ** $p < 0.01$, *** $p < 0.001$, **** $p < 0.0001$, determined by two-tailed Student's t test [Color figure can be viewed at wileyonlinelibrary.com]

4 | DISCUSSION

ER stress and UPR strongly contribute to tumor growth and progression. In PCa, the expression of the UPR components ATF6 α , PERK, and IRE1 α was significantly associated with clinicopathological factors and could predict cancer-specific death. Furthermore, the UPR is sensitive to androgen and favors adaptive responses to promote the survival of PCa cells not only by activating IRE1 α signaling but also by inhibiting the PERK-eIF2 α axis.^{27,28} Further study illustrated that AR signaling and XBP1s coordinate prime proliferating prostate tumor cells for increased protein folding, mRNA decay, and protein translation.²⁹ These facts suggest that selectively manipulating UPR branches may be a therapeutic approach in PCa. ATF6 α is a member of the ATF/cAMP response element-binding protein basic-leucine zipper family of DNA-binding proteins.³⁰ Upon induction of ER stress, ATF6 α directly induces transcriptional activation of ER chaperones and other enzymes, such as glucose-regulated protein 78 (GRP78), which is essential for protein folding.³¹ In this study, we found that overexpression of ATF6 α provides a survival advantage for PCa cells under androgen-deprived or castration conditions, suggesting a critical role of ATF6 α in PCa progression.

ATF6 α is closely related to lipid metabolism, which mediates endoplasmic reticulum proliferation triggered by a membrane protein via phospholipid synthesis.^{32,33} Furthermore, ATF6 α is required for adipogenesis, and ATF6 α -knockout mice display liver steatosis and lipid droplet formation. At the molecular level, ATF6 α interacted with SREBP-2 and subsequently inhibited SREBP2-mediated lipogenesis in HepG2 cells.^{34,35}

ATF6 α also stimulated de novo cholesterol synthesis by upregulating cholesterogenic gene HMGs expression.³⁶ While these studies position ATF6 α as a downstream effector of lipid metabolism, our study is the first to show the direct activation of AA metabolism by increasing the transcriptional output of PLA2G4A. In addition, ATF6 α and PLA2G4A expression was remarkably correlated in human PCa cohorts, further confirming the involvement of ATF6 α -mediated activation of AA metabolism in PCa progression.

PLA2 is a class of enzymes that catalyzes the release of fatty acids from phospholipids. There are several classes of PLA2 in mammals: secreted PLA2, cytosolic PLA2 (cPLA2), calcium-independent PLA2 (iPLA2), lysosomal PLA2, and platelet activation acetylhydrolase (PAF-AH). Considering hydroperoxide phospholipids, ferroptosis is characterized by the accumulation of hydroperoxide phosphatidylethanolamines (Hp-PEs) with a preference for the fatty acyls arachidonoyl (termed HpETE-PE) and adrenoyl (termed HpDTE-PE).^{37–39} Importantly, as a family member of iPLA2, PLA2G6 can hydrolyze Hp-PEs that are implicated in ferroptosis and convert proferroptotic signals into “healthy” membrane phospholipids.⁴⁰ This effect highlights the critical role of PLA2 in ferroptosis. In addition, once activated, PLA2G4A, a member of the cPLA2 family, catalyzes the hydrolysis of membrane phospholipids to release AA, resulting in PGE2 as the end product. Remarkably, PGE2 synergized with *N*-acetylcysteine to prevent hemin-induced ferroptosis. Consistently, our data clearly extend the role of PLA2 in ferroptosis, and PLA2G4A serves as an additional target for preventing excessive ferroptotic death. Here, we also identified ATF6 α as an anti-ferroptotic guardian

by inducing PLA2G4A expression and PGE2 release, thus defining a novel ferroptosis resistance mechanism linking the UPR and lipid metabolism. Consequently, failure of or deficiency in ATF6 α , caused by genetic factors or chemical poisoning, may be associated with increased sensitivity to ferroptotic death.

In the context of PCa, despite differences in available AR-targeted therapies, CRPC cells develop a shared metabolic phenotype in response to AR inhibition. Treatment with enzalutamide induced lipid peroxidation and led to sensitivity to GPX4 inhibition and ferroptosis *in vitro*.⁴ Therefore, the exploitation of ferroptosis for killing cancer cells in response to specific compounds would be helpful for PCa therapy. It has been reported that ferroptosis inducers are effective in inducing ferroptosis in PCa cells.^{41,42} Furthermore, erastin or RSL3 alone or in combination with antiandrogens could act as novel therapeutic strategies for advanced PCa.¹⁵ Therefore, identifying novel factors that could induce ferroptosis may provide additional treatment targets for PCa. ATF6 α has been found to promote the survival of cancer cells and has been linked to cancer development or tumor dormancy. Recently, a novel role of the ATF6 α /PDIA5 axis in regulating resistance to imatinib has also been identified.⁴³ Here, our study showed that the ATF6 α inhibitor Ceapin-A7 synergized with enzalutamide to induce ferroptosis and delayed CRPC progression, thus providing a novel treatment strategy for PCa.

In conclusion, this study reveals the role of ATF6 α -mediated regulation of PLA2G4A activation in ferroptotic resistance. We strengthen the evidence for the critical importance of ferroptosis in PCa, thereby identifying a promising new therapeutic candidate, ATF6 α .

ACKNOWLEDGMENTS

This study was supported by the National Natural Science Foundation of China (Grant Nos. 81772760; 82072850), Taishan Scholar Project of Shandong Province (No. tsqn20161076), The Natural Science Foundation of Shandong Province (Grant Nos. ZR2020YQ55 and ZR2020QH327), The Innovation Project of Shandong Academy of Medical Sciences (2022), The Youth Innovation Technology Plan of Shandong University (2019KJK003), and Academic promotion program of Shandong First Medical University (LJ001).

CONFLICT OF INTERESTS

The authors declare that there are no conflict of interests.

DATA AVAILABILITY STATEMENT

The data that supports the findings of this study are available in the supplementary material of this article.

ORCID

Ru Zhao  <http://orcid.org/0000-0002-7576-2021>

Bo Han  <http://orcid.org/0000-0003-4966-1398>

REFERENCES

1. Viswanathan SR, Ha G, Hoff AM, et al. Structural alterations driving castration-resistant prostate cancer revealed by linked-read genome sequencing. *Cell*. 2018;174(2):433-447.
2. Blomme A, Ford CA, Mui E, et al. 2,4-dienoyl-CoA reductase regulates lipid homeostasis in treatment-resistant prostate cancer. *Nat Commun*. 2020;11(1):2508.
3. Sauer LA, Blask DE, Dauchy RT. Dietary factors and growth and metabolism in experimental tumors. *J Nutr Biochem*. 2007;18(10):637-649.
4. Tousignant KD, Rockstroh A, Poad BLJ, et al. Therapy-induced lipid uptake and remodeling underpin ferroptosis hypersensitivity in prostate cancer. *Cancer Metab*. 2020;8:11.
5. Magtanong L, Ko PJ, To M, et al. Exogenous monounsaturated fatty acids promote a ferroptosis-resistant cell state. *Cell Chem Biol*. 2019;26(3):420-432.
6. Yang WS, Kim KJ, Gaschler MM, Patel M, Shchepinov MS, Stockwell BR. Peroxidation of polyunsaturated fatty acids by lipoxygenases drives ferroptosis. *Proc Natl Acad Sci USA*. 2016;113(34):E4966-E4975.
7. Bebbler CM, Müller F, Prieto Clemente L, Weber J, von Karstedt S. Ferroptosis in cancer cell biology. *Cancers*. 2020;12(1):164.
8. Yang WS, SriRamaratnam R, Welsch ME, et al. Regulation of ferroptotic cancer cell death by GPX4. *Cell*. 2014;156(1-2):317-331.
9. Zhou B, Liu J, Kang R, Klionsky DJ, Kroemer G, Tang D. Ferroptosis is a type of autophagy-dependent cell death. *Semin Cancer Biol*. 2020;66:89-100.
10. Lu J, Yang J, Zheng Y, Chen X, Fang S. Extracellular vesicles from endothelial progenitor cells prevent steroid-induced osteoporosis by suppressing the ferroptotic pathway in mouse osteoblasts based on bioinformatics evidence. *Sci Rep*. 2019;9(1):16130.
11. Gao M, Deng J, Liu F, et al. Triggered ferroptotic polymer micelles for reversing multidrug resistance to chemotherapy. *Biomaterials*. 2019;223:119486.
12. Seibt TM, Proneth B, Conrad M. Role of GPX4 in ferroptosis and its pharmacological implication. *Free Radical Biol Med*. 2019;133:144-152.
13. Sun Y, Qiao Y, Liu Y, et al. ent-Kaurane diterpenoids induce apoptosis and ferroptosis through targeting redox resetting to overcome cisplatin resistance. *Redox Biol*. 2021;43:101977.
14. Roh JL, Kim EH, Jang HJ, Park JY, Shin D. Induction of ferroptotic cell death for overcoming cisplatin resistance of head and neck cancer. *Cancer Lett*. 2016;381(1):96-103.
15. Ghoochani A, Hsu EC, Aslan M, et al. Ferroptosis inducers are a novel therapeutic approach for advanced prostate cancer. *Cancer Res*. 2021;81(6):1583-1594.
16. Almanza A, Carlesso A, Chintha C, et al. Endoplasmic reticulum stress signalling—from basic mechanisms to clinical applications. *FEBS J*. 2019;286(2):241-278.
17. Kaneko M, Imaizumi K, Saito A, et al. ER Stress and disease: toward prevention and treatment. *Biol Pharm Bull*. 2017;40(9):1337-1343.
18. Storm M, Sheng X, Arnoldussen YJ, Saatcioglu F. Prostate cancer and the unfolded protein response. *Oncotarget*. 2016;7(33):54051-54066.
19. Lee YS, Lee DH, Choudry HA, Bartlett DL, Lee YJ. Ferroptosis-induced endoplasmic reticulum stress: cross-talk between ferroptosis and apoptosis. *Mol Cancer Res*. 2018;16(7):1073-1076.
20. Cong L, Ran FA, Cox D, et al. Multiplex genome engineering using CRISPR/Cas systems. *Science*. 2013;339(6121):819-823.
21. Wang L, Li Y, Yang X, et al. ERG-SOX4 interaction promotes epithelial-mesenchymal transition in prostate cancer cells. *Prostate*. 2014;74(6):647-658.
22. Jiang L, Kon N, Li T, et al. Ferroptosis as a p53-mediated activity during tumour suppression. *Nature*. 2015;520(7545):57-62.
23. Wang L, Song G, Tan W, et al. MiR-573 inhibits prostate cancer metastasis by regulating epithelial-mesenchymal transition. *Oncotarget*. 2015;6(34):35978-35990.
24. Wei R, Zhao Y, Wang J, et al. Tagitinin C induces ferroptosis through PERK-Nrf2-HO-1 signaling pathway in colorectal cancer cells. *Int J Biol Sci*. 2021;17(11):2703-2717.

25. Karuppagounder SS, Alin L, Chen Y, et al. N-acetylcysteine targets 5 lipoxygenase-derived, toxic lipids and can synergize with prostaglandin E(2) to inhibit ferroptosis and improve outcomes following hemorrhagic stroke in mice. *Ann Neurol.* 2018;84(6):854-872.
26. Brown N, Morrow JD, Slaughter JC, Paria BC, Reese J. Restoration of on-time embryo implantation corrects the timing of parturition in cytosolic phospholipase A2 group IVA deficient mice. *Biol Reprod.* 2009;81(6):1131-1138.
27. Jin Y, Saatcioglu F. Targeting the unfolded protein response in hormone-regulated cancers. *Trends in Cancer.* 2020;6(2):160-171.
28. Sheng X, Arnoldussen YJ, Storm M, et al. Divergent androgen regulation of unfolded protein response pathways drives prostate cancer. *EMBO Mol Med.* 2015;7(6):788-801.
29. Stelloo S, Linder S, Nevedomskaya E, et al. Androgen modulation of XBP1 is functionally driving part of the AR transcriptional program. *Endocr Relat Cancer.* 2020;27(2):67-79.
30. Hai T, Hartman MG. The molecular biology and nomenclature of the activating transcription factor/cAMP responsive element binding family of transcription factors: activating transcription factor proteins and homeostasis. *Gene.* 2001;273(1):1-11.
31. Ron D, Walter P. Signal integration in the endoplasmic reticulum unfolded protein response. *Nat Rev Mol Cell Biol.* 2007;8(7):519-529.
32. Lagace TA, Ridgway ND. The role of phospholipids in the biological activity and structure of the endoplasmic reticulum. *Biochem Biophys Acta.* 2013;1833(11):2499-2510.
33. Moncan M, Mnich K, Blomme A, Almanza A, Samali A, Gorman AM. Regulation of lipid metabolism by the unfolded protein response. *J Cell Mol Med.* 2021;25(3):1359-1370.
34. Yamamoto K, Takahara K, Oyadomari S, et al. Induction of liver steatosis and lipid droplet formation in ATF6alpha-knockout mice burdened with pharmacological endoplasmic reticulum stress. *Mol Biol Cell.* 2010;21(17):2975-2986.
35. Pullikotil P, Vincent M, Nichol ST, Seidah NG. Development of protein-based inhibitors of the proprotein of convertase SKI-1/S1P: processing of SREBP-2, ATF6, and a viral glycoprotein. *J Biol Chem.* 2004;279(17):17338-17347.
36. Maruyama R, Kamoshida Y, Shimizu M, Inoue J, Sato R. ATF6 α stimulates cholesterol synthesis. *Biosci Biotechnol Biochem.* 2013;77(8):1734-1738.
37. Viswanathan VS, Ryan MJ, Dhruv HD, et al. Dependency of a therapy-resistant state of cancer cells on a lipid peroxidase pathway. *Nature.* 2017;547(7664):453-457.
38. Hadian K, Stockwell BR. SnapShot: Ferroptosis. *Cell.* 2020;181(5):1188.
39. Stockwell BR, Friedmann Angeli JP, Bayir H, et al. Ferroptosis: a regulated cell death nexus linking metabolism, redox biology, and disease. *Cell.* 2017;171(2):273-285.
40. Beharier O, Tyurin VA, Goff JP, et al. PLA2G6 guards placental trophoblasts against ferroptotic injury. *Proc Natl Acad Sci USA.* 2020;117(44):27319-27328.
41. Zhang Y, Guo S, Wang S, et al. LncRNA OIP5-AS1 inhibits ferroptosis in prostate cancer with long-term cadmium exposure through miR-128-3p/SLC7A11 signaling. *Ecotoxicol Environ Saf.* 2021;220:112376.
42. Li M, Chen X, Wang X, et al. RSL3 enhances the antitumor effect of cisplatin on prostate cancer cells via causing glycolysis dysfunction. *Biochem Pharmacol.* 2021;192:114741.
43. Higa A, Taouji S, Lhomond S, et al. Endoplasmic reticulum stress-activated transcription factor ATF6 α requires the disulfide isomerase PDIA5 to modulate chemoresistance. *Mol Cell Biol.* 2014;34(10):1839-1849.

SUPPORTING INFORMATION

Additional supporting information may be found in the online version of the article at the publisher's website.

How to cite this article: Zhao R, Lv Y, Feng T, et al. ATF6 α promotes prostate cancer progression by enhancing PLA2G4A-mediated arachidonic acid metabolism and protecting tumor cells against ferroptosis. *The Prostate.* 2022; 82:617-629. doi:10.1002/pros.24308